Atmos. Chem. Phys., 24, 11029–11043, 2024
https://doi.org/10.5194/acp-24-11029-2024

Atmospheric Chemistry and Physics
Open Access
EGU

Atmospheric evolution of environmentally persistent free radicals in the rural North China Plain: effects on water solubility and $PM_{2.5}$ oxidative potential

Xu Yang[1], Fobang Liu[1], Shuqi Yang[1], Yuling Yang[2], Yanan Wang[1], Jingjing Li[2], Mingyu Zhao[2], Zhao Wang[1,3], Kai Wang[2], Chi He[1], and Haijie Tong[4]

[1]Department of Environmental Science and Engineering, School of Energy and Power Engineering, Xi'an Jiaotong University, Xi'an, Shaanxi 710049, China
[2]State Key Laboratory of Nutrient Use and Management, College of Resources and Environmental Sciences, National Academy of Agriculture Green Development, National Observation and Research Station of Agriculture Green Development (Quzhou, Hebei), China Agricultural University, Beijing 100193, China
[3]Shaanxi Provincial Land Engineering Construction Group Co., Ltd., Xi'an, Shaanxi 710075, China
[4]Institute of Surface Science, Helmholtz-Zentrum Hereon, Max-Planck-Str. 1, 21502 Geesthacht, Germany

Correspondence: Fobang Liu (fobang.liu@xjtu.edu.cn) and Haijie Tong (haijie.tong@hereon.de)

Received: 30 May 2024 – Discussion started: 13 June 2024
Revised: 6 August 2024 – Accepted: 14 August 2024 – Published: 2 October 2024

Abstract. Environmentally persistent free radicals (EPFRs) represent a novel class of hazardous substances, posing risks to human health and the environment. In this study, we investigated the EPFRs in ambient fine, coarse, and total suspended particles ($PM_{2.5}$, PM_{10}, and TSPs) in the rural North China Plain, where local primary emissions of EPFRs were limited. We observed that the majority of EPFRs occurred in $PM_{2.5}$. Moreover, distinct seasonal patterns and higher g factors of EPFRs were found compared to those in urban environments, suggesting unique characteristics of EPFRs in rural areas. The source apportionment analyses revealed atmospheric oxidation as the largest contributor (33.6 %) to EPFRs. A large water-soluble fraction (35.2 %) of EPFRs was determined, potentially resulting from the formation of more oxidized EPFRs through atmospheric oxidation processes during long-range or regional transport. Additionally, significant positive correlations were observed between EPFRs and the oxidative potential of water-soluble $PM_{2.5}$ measured by dithiothreitol-depletion and hydroxyl-generation assays, likely attributable to the water-soluble fractions of EPFRs. Overall, our findings reveal the prevalence of water-soluble EPFRs in rural areas and underscore the fact that atmospheric oxidation processes can modify their properties, such as increasing their water solubility. This evolution may alter their roles in contributing to the oxidative potential of $PM_{2.5}$ and potentially also influence their impact on climate-related cloud chemistry.

1 Introduction

Environmentally persistent free radicals (EPFRs) are a new class of risk substances that have garnered significant attention in recent years (Yi et al., 2023; Vejerano et al., 2018). Unlike short-lived radicals, EPFRs are characterized by their stability, with lifetimes ranging from days to months and even being indefinite (Gehling and Dellinger, 2013; Runberg et al., 2020). They have been identified in various environmental matrices, including soil, sediment, leaves, industrial fly ash, household dust, and atmospheric particulate matter (PM) (Jia et al., 2017; Vejerano and Ahn, 2023; Zhao et al., 2019b; Filippi et al., 2022; Arangio et al., 2016). Of particular interest is their presence in inhalable atmospheric PM, which serves as a crucial carrier for EPFRs, amplifying their detrimental health impacts. Toxicological studies have demonstrated that EPFRs can induce lung damage by triggering oxidative stress in lung cells, primarily through the

reactive oxygen species (ROS) generated from the catalytic cycling of EPFRs (Wang et al., 2011; Balakrishna et al., 2009; Yi et al., 2023). Moreover, the persistent nature of EPFRs and their activation potential by certain environmental factors (e.g., water molecules and ultraviolet light) enable them to participate in diverse atmospheric reactions, initiating or propagating subsequent radical reactions (Truong et al., 2010; Sarmiento and Majestic, 2023; Comandini et al., 2012). Thus, understanding the sources and properties of EPFRs is essential for assessing their atmospheric and health impacts.

The occurrence of EPFRs was initially detected in aerosols originating from cigarette smoke (Pryor et al., 1983) and later also in combustion-derived particles as well as ambient PM (Dalal et al., 1991). Various combustion and thermal processes, including industrial processes, coal combustion, biomass burning, engine exhaust, and waste incineration, have been identified as important sources of EPFRs (Liu et al., 2021; Yang et al., 2017; C. Wang et al., 2020). Mechanistic studies suggest that EPFRs can be generated and stabilized on the surfaces of transition-metal-doped particles in the post-flame and cool-zone regions of combustion systems (Cormier et al., 2006). In addition, secondary chemical processes of organic molecules may also contribute to the presence of EPFRs in atmospheric PM (Chen et al., 2019; C. Wang et al., 2020). Previous work has shown that EPFRs can be formed through the oxidation of organic molecules by ozone and photochemical reactions of PM (Borrowman et al., 2016; Sarmiento and Majestic, 2023; Qin et al., 2021; Tong et al., 2018). Various factors, including solar irradiation, humidity, and the types of precursors, may influence the formation of secondary EPFRs (Sarmiento and Majestic, 2023; Chen et al., 2019; Liu et al., 2023).

Multiple studies conducted in recent decades have investigated the composition of EPFRs in atmospheric PM (Yang et al., 2017; Arangio et al., 2016; Xu et al., 2020). The identified types of EPFRs include carbon-centered and oxygen-centered free radicals, as well as carbon-centered free radicals with a nearby heteroatom. These radicals often manifest as cyclopentadienyl, semiquinone, and phenoxyl radicals (Ai et al., 2023). Notably, Chen et al. (2018b) revealed that the dominant fraction of EPFRs existed within nonsolvent-extractable (unable to be extracted by water, methanol, dichloromethane, and *n*-hexane) organic matter of urban $PM_{2.5}$, underscoring the need for further exploration into the organic molecules associated with ambient EPFRs.

EPFRs exhibit redox activity, capable of reducing oxygen and facilitating the formation of ROS, such as hydroxyl radicals (•OH) and superoxide radicals (O_2^-•) (Hwang et al., 2021; Guo et al., 2020). Consequently, EPFRs may serve as crucial hazardous components contributing to the toxicity of atmospheric PM. Li et al. (2023) found that EPFRs can contribute to the oxidative toxicity of both water-soluble and water-insoluble fractions of atmospheric PM. The types of EPFRs and their extractability may influence their roles in ROS formation (Zhao et al., 2019b). Moreover, ambient EPFRs have been detected in both fine and coarse particles, with observed seasonal and spatial variations in their size distribution (Jia et al., 2023; Wang et al., 2022). The presence of EPFRs in different particle sizes may pose various health risks to humans due to differences in deposition efficiency within the respiratory tract.

The investigations of airborne EPFRs in urban areas, heavily influenced by traffic, industrial, and residential emissions, have been the primary focus of previous studies (Yang et al., 2017; C. Wang et al., 2020). However, EPFRs, characterized by their long lifetimes, can undergo transport over considerable distances and reach rural areas with minimal local emissions. Indeed, the long-range transport of EPFRs has been demonstrated (Chen et al., 2018a). During the transport, the characteristics of EPFRs may undergo evolution through atmospheric chemical processes, potentially altering their roles in ROS formation. Despite this, investigations into the characteristics of airborne EPFRs in areas with limited local emissions remain sparse. Insights into airborne EPFRs in such areas will allow a better understanding of the atmospheric transformation and fate of EPFRs, as well as their atmospheric and health effects.

Therefore, to enhance our understanding of EPFR evolution during atmospheric transport and its effects on ROS formation by the corresponding PM, we collected yearlong PM samples in a typical rural area located in the North China Plain (NCP), where local combustion emissions contributing to EPFRs are minimal. In addition, northern China, including the NCP, is one of the most polluted regions in China, characterized by significant combustion sources, making the selected location ideal for our research objectives. Specifically, our study aims to (i) investigate the characteristics of EPFRs, including their concentration, size distribution, and seasonal variations in the studied region; (ii) determine the sources of EPFRs; and (iii) explore the roles of EPFRs' speciation in contributing to the oxidative potential (OP) of PM.

2 Methods

2.1 PM sample collection

Ambient PM samples were collected at a rural site (36°51′48″ N, 115°00′58″ E) in the county of Quzhou in the NCP from April 2022 to March 2023. The sampling site represents a typical rural environment, predominantly surrounded by croplands and devoid of significant local industrial sources (Fig. S1 in the Supplement). Sequential 24 h fine, coarse, and total suspended particles ($PM_{2.5}$, PM_{10}, and TSPs) were collected using a high-volume sampler (TH-1000CII, Tianhong, China) at a flow rate of $1.05\,m^3\,min^{-1}$. The PM samples were collected onto prebaked (900 °C) quartz filters (Munktell, type MK360) and stored at −20 °C until analysis. In total, 95 PM samples were collected during the whole sampling period. A summary of the number

of $PM_{2.5}$, PM_{10}, and TSP samples collected in each season is provided in Table S1 in the Supplement. In addition, data of other air quality parameters (SO_2, NO_2, O_3, and CO) were obtained from the monitoring site nearest to the sampling site from the local environmental monitoring center.

2.2 EPFR analysis

Three punches (1.2 cm^2 per punch) of each filter were inserted into a quartz tube (5 mm i.d., SP Wilmad-LabGlass) for EPFR measurements using an electron paramagnetic resonance (EPR) spectrometer (A300-9.5/12, Bruker). The detection parameters for EPFRs were set as follows: a modulation frequency of 100 kHz, a microwave frequency of 9.8485 GHz, a microwave power of 1.76 mW, a modulation amplitude of 1.00 G, a sweep width of 150 G, a time constant of 81.92 ms, and a receiver gain of 1×10^3 G. All EPR measurements were conducted at room temperature. To minimize noise in EPR signals, a baseline correction was performed, followed by fitting the signals using a Gaussian function via the least-squares method. EPFR concentrations for the filters were determined by comparing the peak area with a calibration curve (Fig. S2) generated using a common radical stand, 4-hydroxy-2,2,6,6-tetramethylpiperidine-1-oxyl (TEMPOL) (Arangio et al., 2016).

In addition, we conducted water extraction and acidification experiments on the samples to determine the reduction of EPFR contents on the filter samples after treatment. The procedures of water extraction and acidification were adopted from previous studies (Chen et al., 2018b; Yang et al., 2017). For water extraction, all $PM_{2.5}$ samples were processed alongside two randomly selected PM_{10} and TSP samples from each season. Briefly, three punches (1.2 cm^2 per punch) of each filter were immersed in 3 mL of deionized water for 14 h under dark conditions. Regarding acidification, two $PM_{2.5}$, PM_{10}, and TSP samples in each season were randomly selected, and two punches (1.2 cm^2 per punch) of each filter were immersed in 2 mL of 6 M HCl solution for 1 h under dark conditions. Subsequently, the filter punches were dried by a vacuum freeze dryer before conducting EPFRs measurements using the aforementioned detection parameters. All the EPFR measurements were conducted within 1 year of sampling.

2.3 Carbonaceous fractions and element analyses

A 1.0 cm^2 punch of each sample filter was analyzed for organic carbon (OC) and elemental carbon (EC) following the Interagency Monitoring of Protected Visual Environments (IMPROVE) thermal–optical reflectance (TOR) protocol using the DRI model 2001 carbon analyzer. Different carbonaceous fractions, including OC1–OC4 and EC1–EC3, were isolated and quantified based on their thermal stability.

A total of 12 elements (Li, Mg, Al, Si, K, Ca, Cr, Mn, Fe, Cu, Zn, and Pb) were analyzed using inductively coupled plasma mass spectrometry (ICP-MS; Thermo Scientific iCAP RQ). Prior to analysis, a 3.6 cm^2 punch of each filter was digested using 1 mL of aqua regia ($HNO_3 + 3HCl$, $v : v$) at 99 °C and a rotational frequency of 350 rpm for 24 h. After digestion, the extracts were filtered through a 0.22 µm PTFE syringe filter and then diluted to 5 mL deionized water with 2 % HNO_3.

2.4 Oxidative potential measurements

The OP of PM samples was measured by two techniques, the dithiothreitol-depletion assay and •OH-production assay (Verma et al., 2012; Son et al., 2015). In the dithiothreitol (DTT) assay, the decay of 100 µM DTT by PM in phosphate buffer was monitored over a 40 min incubation at 37 °C. The remaining DTT after the incubation was quantified by its reaction with dithiodinitrobenzoic acid, yielding ultraviolet-detectable 2-nitro-5-thiobenzoic acid (Verma et al., 2012; Fang et al., 2015). In the •OH-production assay, the terephthalate (10 mM) in phosphate buffer was used to measure •OH formation by PM throughout 2 h incubation at 37 °C. At pH 7.4, terephthalate reacted with •OH to form stable and highly fluorescent hydroxyterephthalic acid (2-OHTA), and the production rate of •OH was calculated based on the produced 2-OHTA, as the formation of 2-OHTA is proportional to the generation of •OH (Yu et al., 2022; Li et al., 2019). Note that samples were incubated at a PM concentration of 100 µg mL^{-1} for both assays. Meanwhile, both total OP (Total-OP) and water-soluble OP (WS-OP) were determined in this work. For total OP determination, unfiltered PM extracts with filter punches left in the extracts were directly incubated with the probes, while for water-soluble OP, the extract was filtered through a 0.22 µm PTFE syringe filter before incubating with probes. The OP contribution from water-insoluble PM components (water-insoluble OP, WIS-OP) was considered the difference between Total-OP and WS-OP. A detailed description of the DTT and •OH assays can be found in the Supplement (Sect. S1).

2.5 Statistical analysis

2.5.1 Positive matrix factorization

The EPA positive matrix factorization (PMF 5.0) model was employed to apportion the sources of EPFRs and PM in this study. The PMF model is an advanced multivariate factor analysis tool widely utilized for source apportionment of environmental pollutants (Heo et al., 2013; Wang et al., 2019). The input data include the concentrations and uncertainties of PM, EPFRs, organic carbon fractions (OC1, OC2, OC3), elemental carbon fractions (EC1, EC2, EC3), SO_2, NO_2, CO, O_3, and the 12 elements. The uncertainties of each variable were calculated using the following equation: uncertainty $= K \times$ concentration, where K denotes analytical uncertainty (Wang et al., 2019). For PM, EPFRs, OC, and EC, K was set as 10 % (Jang et al., 2020). For metal elements and

meteorological parameters, K was set as 15 % (Ikemori et al., 2021). Missing values and associated uncertainties were estimated by substituting the median concentrations of the components and 4 times the median value of the components to mitigate their impact on the results (Wang et al., 2019).

The PMF model was run with four to seven factors and with random seeds. The six-factor result was considered the optimal one based on a minimal Q value (indicating the variation between the observation and the model is the least), $Q_{\text{Robust}}/Q_{\text{Theo}}$ (< 2), scaled residuals (within ± 3), and the interpretable profiles from the literature (Reff et al., 2007; Ramadan et al., 2000). Bootstrap and displacement analyses were conducted to estimate the uncertainty of the PMF model with six factors (Brown et al., 2015), and the results are shown in Fig. S3. The bootstrap factor mapping exceeded 93 % for all factors without any displacement run exchanges.

2.5.2 Correlation analysis

Correlation analysis was performed using Pearson's correlation coefficients and two-tailed significance tests by IBM SPSS Statistics 27.

2.6 Backward trajectories

To characterize the origins and transport pathways of the air masses to the sampling site, 48 h backward trajectories of the air masses were simulated using the Hybrid Single-Particle Lagrangian Integrated Trajectory (HYSPLIT) model. The input meteorological data were acquired from the Global Data Assimilation System (ftp://arlftp.arlhq.noaa.gov/pub/archives/gdas1, last access: 7 April 2023).

3 Results and discussion

3.1 Characteristics of EPFRs in different sizes of PM

Figure 1a illustrates the box plots of volume-normalized (EPFRv) concentrations of EPFRs in different sizes of PM during the entire sampling. EPFRv levels in $PM_{2.5}$, averaging $(5.6 \pm 1.1) \times 10^{12}$ spins m^{-3}, accounted for over 95.2 % of those in PM_{10} ($(5.8 \pm 1.0) \times 10^{12}$ spins m^{-3}) and TSPs ($(5.9 \pm 1.1) \times 10^{12}$ spins m^{-3}). However, the average mass concentration of $PM_{2.5}$ only represented 61.8 % of that in PM_{10} and 47.5 % of that in TSPs (Fig. S4). Similar results were found for EPFRv and PM concentrations in each season (Fig. S5). These results suggest that the majority of airborne EPFRs are present in $PM_{2.5}$, with only a small portion occurring in the 2.5–10 µm size range.

This is further evident by the results of mass-normalized (EPFRm) concentration of EPFRs, as depicted in Fig. 1b. The average EPFRm in $PM_{2.5}$ $(6.5 \pm 3.5) \times 10^{16}$ spins g^{-1}) was approximately 1.7 times that in PM_{10} ($(3.9 \pm 2.1) \times 10^{16}$ spins g^{-1}) and 2.2 times that in TSPs ($(3.0 \pm 1.7) \times 10^{16}$ spins g^{-1}). Consistent with our finding, previous studies have also observed a predominant fraction of EPFRs in smaller sizes (< 2.5 µm) of PM (Chen et al., 2020; Dugas et al., 2016). The strong association of EPFRs with fine particles may stem from multiple factors. Firstly, airborne EPFRs primarily originate from the combustion of organic materials and multiphase chemistry of gaseous organics in the atmosphere, processes that predominantly form fine particles (Tian et al., 2009; Arangio et al., 2016). Additionally, the larger specific surface area and porous structure of fine particles facilitate the attachment of EPFRs, leading to their higher retention within this fraction (Yang et al., 2017).

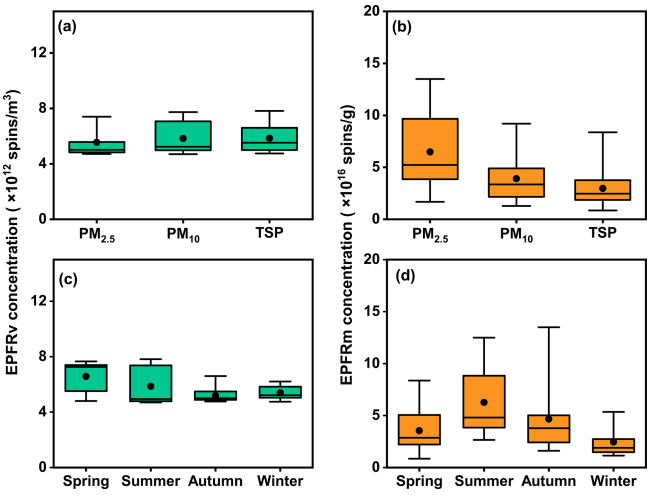

Figure 1. The concentrations of EPFRv **(a, c)** and EPFRm **(b, d)** in different sizes of PM samples and different seasons. The boxes represent the 25th percentile (lower edge), median (solid line), mean (solid dot), and 75th percentile (upper edge). The whiskers represent the minimum and maximum.

Table S2 presents a summary of the concentrations of EPFRv and EPFRm in this study compared to the existing literature. Both EPFRv and EPFRm in this study were lower than in most urban and suburban environments (Wang et al., 2019; Jia et al., 2023; Yang et al., 2017). This implies that there were only limited local sources directly emitting EPFRs at this rural site. This is further supported by the seasonal variation of EPFRs. Notably, higher EPFRv levels were observed in summer than in winter (Fig. 1c), with the highest EPFRm occurring during summer (Fig. 1d) in the studied area. This contrasts with findings from previous studies, which indicated that winter typically exhibits the highest EPFRv, especially for cities in northern China with prominent local emission sources of EPFRs, such as large-scale coal consumption (Wang et al., 2019; Jia et al., 2023; Ai et al., 2023). The distinct seasonal characteristic of EPFRs observed in our study could be attributed to the limited residential and industrial activities in the rural NCP. On the other hand, the highest EPFRm levels in summer may be linked to enhanced atmospheric oxidation, promoting EPFR formation

due to elevated concentrations of photooxidants and stronger solar irradiation (Borrowman et al., 2016; Sarmiento and Majestic, 2023; Shiraiwa et al., 2011).

In addition to examining the concentrations of EPFRs, we also investigated the g factors of EPFRs across different sizes of PM, as the g factor is an important indicator of EPFR characteristics. We observed that the g factors for all PM samples ranged between 2.0033 and 2.0037, with a mean value of 2.0035 ± 0.0001 (Fig. S6). These g factors are higher than the values obtained from PM samples collected from highway and urban locations (Hwang et al., 2021; Fang et al., 2023). A g factor below 2.003 signifies the presence of carbon-centered radicals (e.g., cyclopentadienyl), while a g factor exceeding 2.004 indicates oxygen-centered radicals (e.g., phenoxy, semiquinone radicals). A g factor falling between 2.003–2.004 suggests a carbon-centered radical with adjacent oxygen atoms (Ai et al., 2023; Yang et al., 2017). The observed g factors in this work indicate the presence of carbon-centered radicals with adjacent oxygen atoms and oxygen-centered radicals. Furthermore, we noted a decreasing trend in the g factor with particle size (i.e., $PM_{2.5} > PM_{10} > TSPs$), indicating closer proximity of the unpaired electron to the oxygen center in smaller particles. This trend could be attributed to the increased exposure of porous structures in smaller particles, rendering them more susceptible to oxidation (Yang et al., 2017).

3.2 Sources of EPFRs

The PMF analysis was utilized to identify and quantify the sources contributing to EPFRs. As shown in Fig. 2a, six primary source factors were determined. Factor 1 was attributed to atmospheric oxidation, characterized by its elevated proportion of O_3. The presence of O_3 signifies atmospheric oxidative capability (Ainur et al., 2023; Y. Q. Wang et al., 2020). Factor 2 exhibited high proportions of Al, Fe, Cr, SO_2, CO, and EC, suggesting industrial emissions. Al and Fe could be associated with iron and steel production and the metal industry (Khobragade and Ahirwar, 2022). The availability of Cr is linked to fossil fuel combustion or oil combustion (Alleman et al., 2010; Begum et al., 2011). SO_2 and CO are typical tracers of coal combustion (Johnson et al., 2006; Kundu et al., 2010; Wang et al., 2019), and they (and also EC) could be emitted from coal-based industries. Factor 3, characterized by high proportions of SO_2, NO_2, and CO, was identified as coal combustion (Johnson et al., 2006; Kundu et al., 2010; Wang et al., 2019). Previous research indicates that NO_2 emissions, although often associated with vehicle emissions, are also prevalent in coal combustion (Ainur et al., 2023; Lei et al., 2016; C. A. Wang et al., 2018). In factor 4, high proportions of OC3, OC4, EC1, EC2, EC3, Mn, Cu, and Pb were observed, suggesting motor vehicle emissions. EC1, OC2, OC3, and OC4 primarily originate from gasoline vehicle emissions, while EC2 and EC3 are closely associated with diesel vehicle emissions (Kim and Hopke, 2004; Ai et al., 2023). Additionally, Mn (from unleaded gasoline additives), Pb (from gasoline additives), and Cu (from brake linings) contribute to this factor (Sharma et al., 2014). Factor 5 displayed a high loading of OC1 and a considerable loading of OC2, indicative of biomass burning. OC1 and OC2 have been linked to biomass combustion in previous studies (Stanimirova et al., 2023; Cao et al., 2005; Dong et al., 2022). Factor 6 exhibited high proportions of Mg and Ca, indicative of soil dust as these elements are major constituents of the Earth's crust (An et al., 2015; Y. Liu et al., 2022).

In summary, the six primary sources contributing to EPFRs were identified as atmospheric oxidation, industrial emissions, coal combustion, motor vehicle emissions, biomass burning, and soil dust. As shown in Fig. 2b, atmospheric oxidation emerged as the largest contributor (33.6 %) to EPFRs during the entire sampling period. The formation of EPFRs through atmospheric oxidation could occur via photooxidant oxidation (reactions of polycyclic aromatic hydrocarbons (PAHs) with solar radiation, O_3, and •OH) and metal-catalyzed redox reaction (PAHs interacting with metals under visible and UV light irradiation). Solar radiation and O_3 can directly generate EPFRs by disrupting the stable covalent bonds of organic substances, while metals act as electron acceptors, facilitating electron transfer with PAHs to form EPFRs, as suggested by previous studies (Borrowman et al., 2016; Shiraiwa et al., 2011; Chen et al., 2019; C. Wang et al., 2020).

The significant contribution of atmospheric oxidation observed in our study contrasts with findings from urban areas, where primary sources typically dominate airborne EPFRs (Ainur et al., 2023, 2022). The results of seasonal source apportionments (Fig. 2b) further illustrate much higher contributions of atmospheric oxidation in spring (42.2 %) and summer (50.3 %) compared to autumn (21.3 %) and winter (18.6 %). The elevated contribution in summer aligned with the expectation of stronger photochemistry. The relatively high contribution in spring could be attributed to the dominance of long-range transport of air mass (60 %, Fig. S7a), which was markedly higher than the proportions (< 23 %) observed in the other seasons. Previous studies have suggested that long-range transport of air mass favors atmospheric oxidation occurrence more than the air mass from regional/short-range transport (Ramya et al., 2023; Zhong et al., 2022).

Industrial emissions (30.8 %) were the second-largest contributor to annual EPFRs, followed by coal combustion (14.5 %), motor vehicle emissions (10.3 %), biomass burning (6.6 %), and soil dust (4.2 %). Industrial emissions and coal combustion have been widely suggested as significant sources of EPFRs (C. Wang et al., 2020; Yang et al., 2017; P. Wang et al., 2018). Although industrial activities were limited at this rural site, emissions might originate from surrounding industrial cities such as Handan in the south, as indicated by backward trajectory analysis (Fig. S7). Over 17 % of air mass was identified as regional transport from

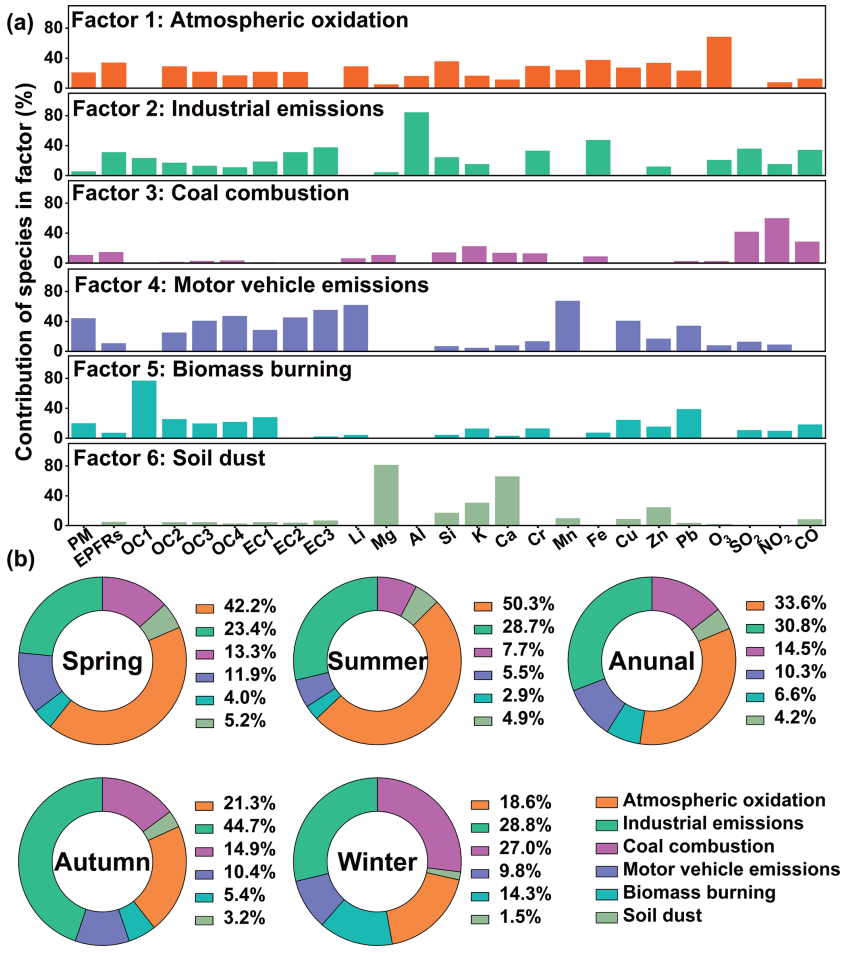

Figure 2. **(a)** Factor profile obtained by positive matrix factorization analysis. **(b)** Seasonal and annual contributions of the six factors to EPFRs.

the south, particularly notable in autumn (54 %), corresponding to a higher contribution (44.7 %) of industrial emissions to EPFRs compared to other seasons. Winter exhibited notably higher contributions from coal combustion and biomass burning, as coal and biomass are primary fuels for residential heating in the rural NCP during this season.

While motor vehicle emissions accounted for a small contribution to EPFRs, they constituted the largest contributor (43.8 %) to PM (Fig. S8), suggesting differing components contribute to EPFRs and PM. For instance, volatile organic compounds (e.g., toluene) and nitrogen oxides emitted from vehicle exhausts may significantly contribute to PM formation but are generally not considered major contributors to EPFRs (Nagpure et al., 2016; Gao et al., 2022; Wang et al., 2019). Regarding soil dust, recent studies indicate that PAHs readily adsorb on mineral surfaces, likely forming "cation–π" interactions with active sites. This interaction promotes electron transfer from aromatic compounds to surface cations on clay surfaces, facilitating the formation of intermediate radicals/final products (Zhao et al., 2019a; Ni et al., 2023).

3.3 Associations of EPFRs with OP of PM

3.3.1 OP of PM

Oxidative potential, defined as the catalytic generation of ROS by PM components, serves as a plausible metric for assessing PM toxicity (Abrams et al., 2017; Weichenthal et al., 2016; Daellenbach et al., 2020; Bhattu et al., 2024). EPFRs have been identified as significant contributors to the OP of PM due to their ability to catalytically generate ROS (Gehling et al., 2014; Hwang et al., 2021). In this work, we also measured the OP of the PM samples using two commonly used assays: dithiothreitol-depletion (OP^{DTT}) and hydroxyl-generation ($OP^{\bullet OH}$) assays. OP^{DTT} is found to be a good indicator of the production of $O_2^-\bullet$ and H_2O_2 but does not capture •OH generation (Fang et al., 2019). Thus, the combined application of two assays provides complementary insights into the role of EPFRs in ROS generation. Further, WS-OP, WIS-OP, and Total-OP were all determined to explore their potential correlations with EPFRs.

Tables S3 and S4 summarize the OP results in this work. A detailed discussion of OP values between the present work and literature can also be seen in the Supplement (Sect. S2). In short, consistent with the findings of EPFRm, the mass-normalized OP (OPm) values in this work were also lower than in most urban and suburban environments. This disparity suggests fewer redox-active PM components in the studied rural area, likely due to the absence of significant local emission sources of pollutants.

Figure 3a illustrates the box plots of mass-normalized WS-OP, WIS-OP, and Total-OP determined by the two assays. Generally, Total-OP levels were higher than WS-OP and WIS-OP, demonstrating measurable contributions of both water-soluble and water-insoluble species to the overall OP of PM. Additionally, WS-OP accounted for a larger fraction of Total-OP in both assays (WS-OP^{DTT}: 67.8 ± 20.5 %; WS-$OP^{\bullet OH}$: 56.1 ± 22.6 %). Furthermore, a reverse relationship between particle size and the contribution of WS-OP to Total-OP was observed, with the largest contribution in $PM_{2.5}$, followed by PM_{10} and TSPs (Fig. 3b). A significantly higher contribution of WS-OP^{DTT} to Total-OP^{DTT} has also been observed for ambient $PM_{2.5}$ at multiple locations worldwide (Gao et al., 2017; Yang et al., 2024; Li et al., 2024). Yet, PM samples near highways and road dust have shown a higher fraction of WIS-OP^{DTT} than WS-OP^{DTT} (Zhang et al., 2024; Li et al., 2023). This could be due to a lower solubility of PM at the sites near primary emissions. These divergent results suggest that atmospheric oxidation processes may alter the role of PM components in contributing to OP.

3.3.2 Associations among EPFRs, OP, and PM components

To identify individual chemical species influencing the intrinsic redox activity of ambient PM, correlation analyses between mass-normalized OP ($OP^{DTT/\bullet OH}$) and the mass fraction of determined chemical species were performed. The results are shown in Fig. 4, and the detailed information is also listed in Tables S5–S7 (the volume-normalized correlation results are also included in Fig. S9 in the Supplement in case the readers are interested).

Notably, the chemical species associated with Total-OP and WS-OP exhibited similarities, particularly for $PM_{2.5}$ (Fig. 4). This may be partly because Total-OP was primarily comprised of WS-OP (Fig. 3b). Also, good correlations were observed between Total-OP and WS-OP, except for the $OP^{\bullet OH}$ of TSP samples (Fig. S10). In addition, we observed that OP^{DTT} and $OP^{\bullet OH}$ were sensitive to different chemical species (Fig. 4). Specifically, OC, EC, EPFRs, Fe, and Cr showed good correlations with Total-OP^{DTT} and WS-OP^{DTT}, while Cu exhibited a good correlation with Total-$OP^{\bullet OH}$ and WS-$OP^{\bullet OH}$ ($r > 0.5$, $p < 0.05$). As mentioned before, OP^{DTT} is a good indicator of the production of $O_2^{-}\bullet$ and H_2O_2 (Fang et al., 2019). Thus, these results indicate that different chemical species contribute to the production of distinct types of ROS (Campbell et al., 2021; Jin et al., 2019; Calas et al., 2018). In terms of WIS-OP, only OC showed a moderate correlation ($r = 0.43$, $p < 0.05$) with WIS-OP^{DTT}. No species displayed a positively good correlation with WIS-$OP^{\bullet OH}$, implying that WIS-OP might arise from complex synergistic–antagonistic interactions among PM components (Charrier and Anastasio, 2015; Yu et al., 2018). However, further research is warranted to elucidate the mechanisms and PM components responsible for WIS-OP.

Interestingly, EPFRs in $PM_{2.5}$ exhibited significant correlations with WS-OP but not with WIS-OP (Fig. 4). This observation contradicts previous studies reporting that the majority of EPFRs are not water-extractable (Chen et al., 2018b; Guo et al., 2023; P. Wang et al., 2018). Given the source apportionment results showing atmospheric oxidation as the largest contributor to EPFRs, we hypothesized that atmospheric oxidation processes may have increased the water solubility of rural EPFRs, leading to the observed significant correlations.

3.3.3 Solubility of EPFRs and its linkages with OP

To demonstrate the possibly high solubility of EPFRs, additional experiments were conducted with PM filters extracted by water prior to EPFR analysis. On average, a 35.2 % reduction in EPR signals was observed after water extraction (Fig. 5), indicating that the same percentage of EPFRs was water-soluble (a detailed breakdown of the water-soluble fraction of EPFRs in each filter is listed in Table S8). This result is substantially higher than the reported water-soluble fraction (0.2 %) of EPFRs in urban $PM_{2.5}$ of Xi'an (Fig. 5b), where the majority of EPFRs likely consisted of graphene oxide analogues (Chen et al., 2018b). In addition, the result is also higher than that (11 %) of EPFRs emitted from biomass burning (Guo et al., 2023), suggesting a high water-soluble fraction of EPFRs in the studied rural area.

It is widely acknowledged that EPFRs from combustion processes are formed through the electron transfer mediated by transition metals on organic combustion byproducts such as PAHs (S. T. Liu et al., 2022; Vejerano et al., 2018). The EPR signal of these metal–EPFR complexes can be substantially reduced (> 90 %, Fig. 5c) after acidification, as demonstrated by previous work (Guo et al., 2023). We also conducted the same acidification procedure and observed, on average, a 70 % reduction in EPR signals (Fig. 5c; detailed information is provided in Table S9). Although the reduction in our work is not as substantial as that of biomass burning particles (Guo et al., 2023), the result indicates that there was a large fraction of EPFRs in the form of metal–EPFR complexes, likely originating from combustion sources (e.g., coal and biomass combustion). In addition, EPFRs showed significantly good correlations ($r > 0.5$, $p < 0.01$; Table S10) with certain transition metal species (i.e., Fe, Zn, Cr), suggesting their formation was likely associated with transition metals. The higher water-soluble fraction of EPFRs in our work com-

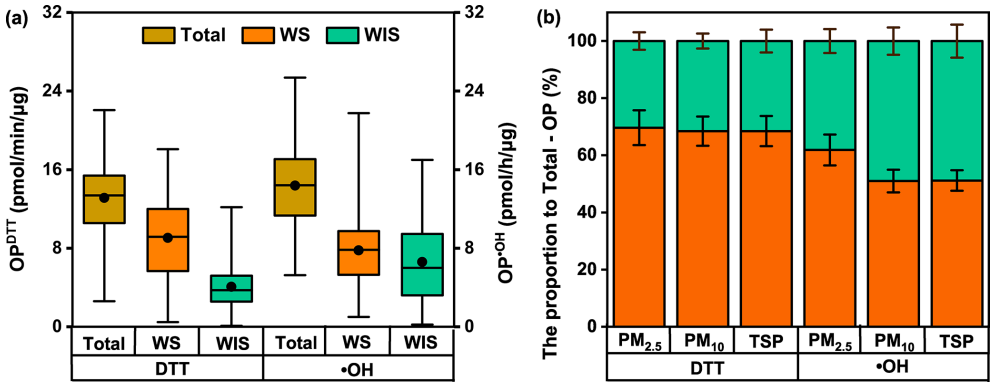

Figure 3. **(a)** The concentrations of total, water-soluble (WS), and water-insoluble (WIS) fractions of OP^{DTT} and $OP^{•OH}$. The boxes represent the 25th percentile (lower edge), median (solid line), mean (solid dot), and 75th percentile (upper edge). The whiskers represent the minimum and maximum. **(b)** Proportions of WS-OP and WIS-OP to Total-OP in different sizes of PM samples; the bar indicates the standard error.

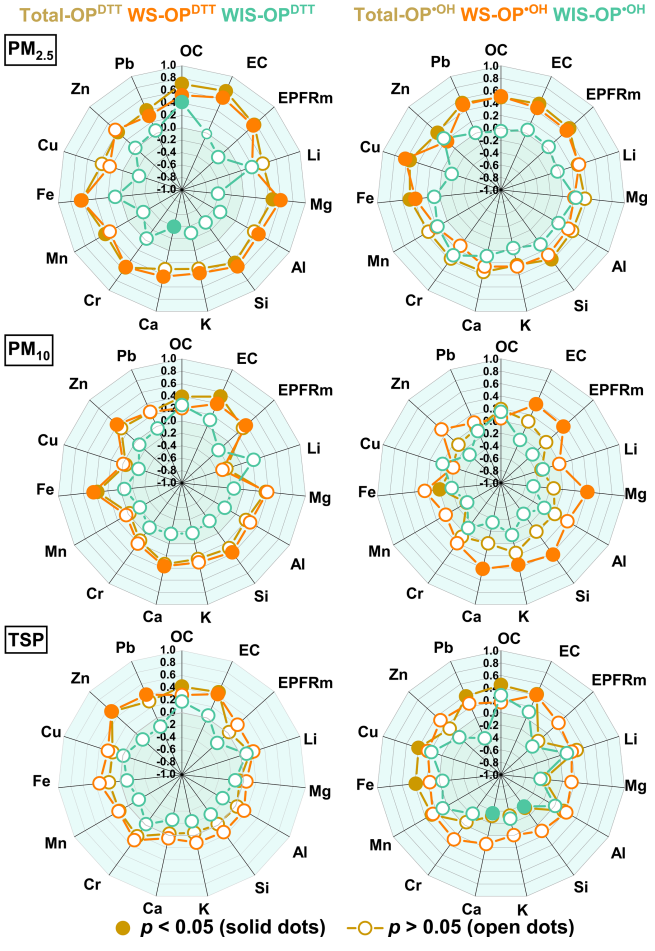

Figure 4. Correlation coefficients (Pearson's r) of mass-normalized OP (Total-OP, WS-OP, and WIS-OP) with mass fractions of selected chemical species.

pared to that of biomass burning particles could be relevant to the increased polarity of EPFRs by atmospheric oxidation processes (i.e., the aging of metal–EPFR complexes). It is also worth noting that the reduction of EPR signals is at a much greater extent than that (24 %, Fig. 5c) of EPFRs (mostly consisting of graphene oxide analogues) in urban $PM_{2.5}$ of Xi'an (Chen et al., 2018b).

In addition to the potentially oxidized/aged metal–EPFR complexes, another significant source of water-soluble EPFRs could be EPFRs directly generated by secondary chemical processes. Chen et al. (2019) found that water-extracted humic-like substances were the primary precursors of secondary EPFRs formed by visible-light illumination in ambient PM. A laboratory study by Tong et al. (2018) demonstrated that secondary organic aerosol formed by photooxidation of naphthalene contained EPFRs at levels comparable to those found in ambient PM. Given that atmospheric oxidation was the main source of EPFRs and PM in our studied region, these secondary chemical processes likely had a substantial impact on ambient PM, contributing to the formation of secondary EPFRs. However, further research is needed to fully elucidate and quantify the contribution of secondary formation pathways to water-soluble EPFRs.

Importantly, compared to total EPFRs, water-soluble EPFRs (WS-EPFRs) showed stronger correlations with WS-OP (Fig. 6) of $PM_{2.5}$. In addition, no significant correlation was observed between water-insoluble EPFRs (WIS-EPFRs) and WS-OP (Fig. S11a and b). These results demonstrate our hypothesis that the significant correlations between EPFRs and WS-OP were driven by the water-soluble fractions of EPFRs, while atmospheric oxidation processes had increased the water solubility of EPFRs. On the other hand, the lack of significant correlation between WIS-EPFRs and WIS-OP (Fig. S11c and d) could be attributed to the complex interplay of organics and metals affecting WIS-OP (Gao et al., 2020). Nonetheless, the significant correlation between WS-

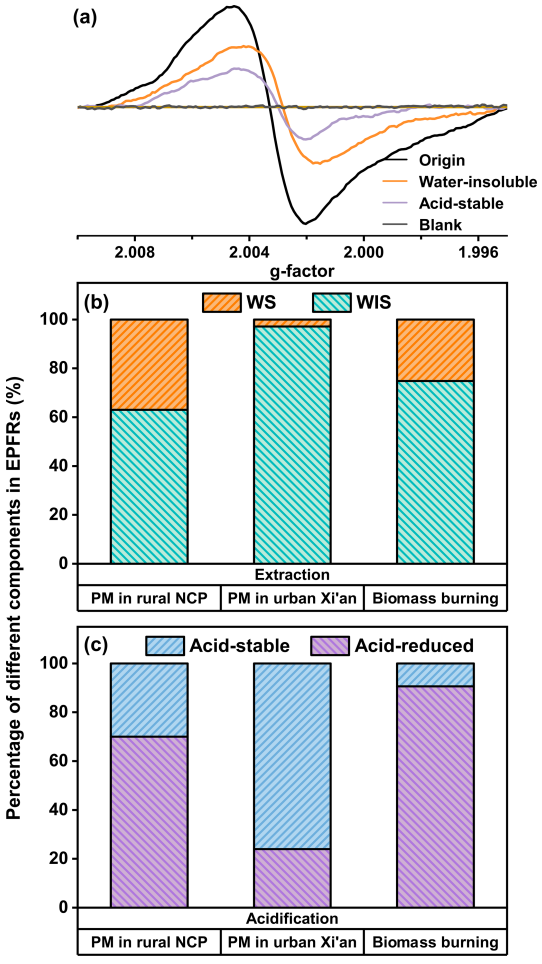

Figure 5. **(a)** Gaussian fitting EPR spectra of a selected $PM_{2.5}$ filter sample (sampling date: 12 March 2023) before (black) and after water extraction (orange), as well as after acidification (purple). A typical EPR spectrum of a blank filter (grey) is also present for reference. **(b)** The percentages of different fractionated EPFRs in the rural NCP (this study), in urban PM of Xi'an (Chen et al., 2018b), and in biomass burning particles (Guo et al., 2023).

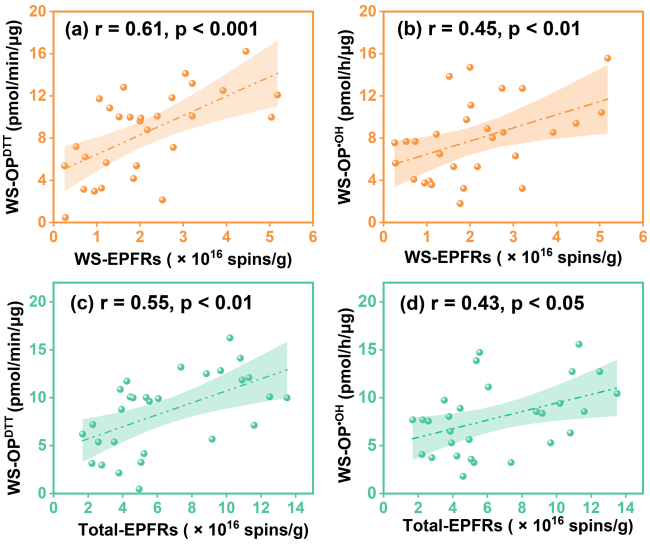

Figure 6. Correlation of WS-EPFRs and Total-EPFRs with WS-OP in $PM_{2.5}$: **(a)** WS-EPFRs with $WS\text{-}OP^{DTT}$, **(b)** WS-EPFRs with $WS\text{-}OP^{\bullet OH}$, **(c)** Total-EPFRs with $WS\text{-}OP^{DTT}$, and **(d)** Total-EPFRs with $WS\text{-}OP^{\bullet OH}$. The Pearson correlation coefficients (r) and associated p values are illustrated in the figure. The lines and shaded areas are linear regressions with their 95 % confidence intervals.

EPFRs and WS-OP suggests that atmospheric oxidation processes may have contributed to the increased water solubility of EPFRs, thereby affecting their roles in $PM_{2.5}$ oxidative potential.

4 Conclusions and implications

In this study, EPFRs in fine, coarse, and total suspended particles in a typical rural region of the NCP have been investigated. The majority of EPFRs occurred in fine particles. EPFRs exhibited seasonal patterns distinct from those observed in urban environments. In addition, higher g factors of EPFRs were identified compared to those reported for highway and urban PM, suggesting a greater extent of oxidation in rural EPFRs. These findings underscore a unique characteristic of EPFRs in rural areas, where local primary emissions of EPFRs are limited.

Additionally, atmospheric oxidation was resolved as the largest contributor to EPFRs. The atmospheric oxidation processes occurring during long-range or regional transport were suggested as the primary driver behind the more oxidized EPFRs observed in our work. We also demonstrated that the rural EPFRs contained a higher water-soluble fraction compared to those found in biomass burning particles and urban PM. Our results thus emphasize the importance of considering the water-soluble fraction of EPFRs, alongside their occurrence in organic solvent-extractable or non-extractable organics, particularly in regions without significant primary emissions of EPFRs. Future studies are warranted to investigate airborne EPFRs in other rural regions to yield a more complete understanding of the sources and properties of EPFRs, as only a typical rural site in the NCP was examined in our work.

The WS-EPFRs could be an important contributor to the oxidative potential of $PM_{2.5}$, as suggested by their significant positive correlations. While prior research has predominantly focused on EPFRs in urban environments or originating from primary combustion emission sources, our findings revealed the evolution of EPFRs through atmospheric oxidation during transport (Fig. 7). The atmospheric evolution of EPFRs may modify their properties, such as water solubility, thereby altering their roles in contributing to the oxidative potential of PM (S. Y. Wang et al., 2018). It is also important to note that water-soluble EPFRs are more bioavailable than their in-

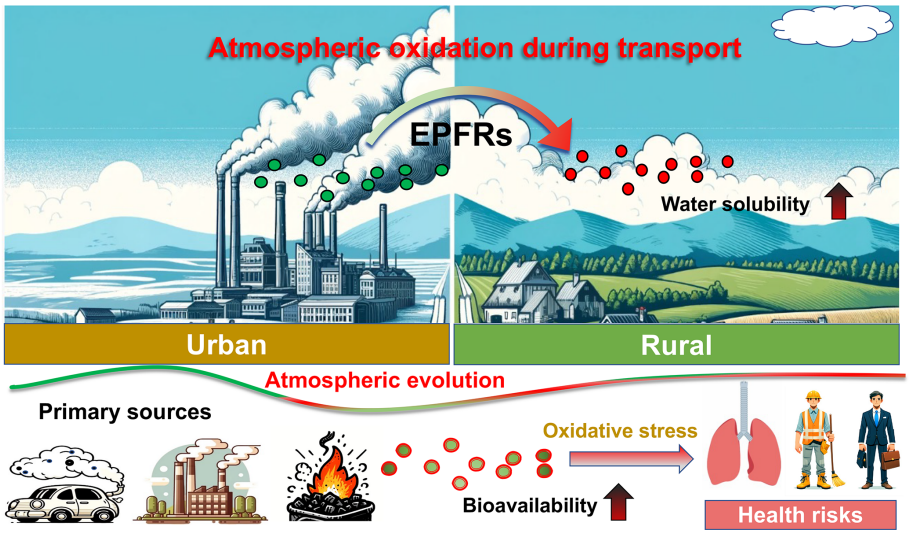

Figure 7. Implication of the atmospheric evolution of EPFRs. EPFRs, primarily emitted from combustion sources, may undergo atmospheric oxidation during long-range or regional transport. This transformation may enhance the water solubility of EPFRs, potentially heightening their bioavailability and consequently elevating risks to human health.

soluble forms. They are more likely to reach the tissues or organs beyond the lung deposition site, amplifying the risk to human health (Liu and Ng, 2023). Furthermore, beyond influencing the oxidative toxicity of PM, the role of evolved EPFRs in climate-related cloud chemistry may also change and should be explored in future research.

Generally, soluble EPFRs are assumed to have a relatively short lifetime. For instance, it has been found that secondary EPFRs formed by photoexcitation are highly susceptible to reduction by oxygen, leading to short lifetimes ranging from approximately 30 min to 1 d (Chen et al., 2019). However, measurements conducted on several $PM_{2.5}$ filters stored at −20 °C for roughly 1 year showed that EPR signals only decreased by approximately 11 % (Fig. S12), suggesting the persistency of EPFRs, including their water-soluble fraction. Previous research has indicated that semiquinone-type radicals adsorbed into a polymeric carbonaceous core (Valavanidis et al., 2005) or by electron transfer with transition metals (Truong et al., 2010) are stable and can have a lifetime longer than months. However, their water solubility remains unclear. Further efforts to identify the types of water-soluble EPFRs and investigate their lifetimes are warranted.

Overall, this study revealed the characteristics of EPFRs in rural regions, highlighting the importance of considering atmospheric oxidation processes in understanding their behavior and impacts. Future research efforts should aim to further elucidate the mechanisms governing the formation, evolution, and fate of EPFRs, as well as their interactions with other atmospheric components. Such insights are essential for developing effective strategies to mitigate the adverse effects of EPFRs on air quality and public health, as well as for advancing our understanding of their broader implications for atmospheric and environmental science.

Data availability. The data are available upon request to the corresponding authors Fobang Liu (fobang.liu@xjtu.edu.cn) and Haijie Tong (haijie.tong@hereon.de).

Supplement. The supplement related to this article is available online at: https://doi.org/10.5194/acp-24-11029-2024-supplement.

Author contributions. FL and XY designed the research. XY, SY, YY, YW, JL, MZ, and ZW carried out the experiments. FL, CH, HT, and KW supervised the study. FL and XY prepared the original manuscript with input from all the co-authors.

Competing interests. The contact author has declared that none of the authors has any competing interests.

Disclaimer. Publisher's note: Copernicus Publications remains neutral with regard to jurisdictional claims made in the text, published maps, institutional affiliations, or any other geographical representation in this paper. While Copernicus Publications makes every effort to include appropriate place names, the final responsibility lies with the authors.

Acknowledgements. We gratefully acknowledge technical support from Professor Station of China Agricultural University at Xinzhou Center for Disease Control and Prevention. We acknowledge the use of ChatGPT 4.0 to generate the cartoons of Fig. 7.

Financial support. This research has been supported by the Natural Science Basic Research Program of Shaanxi Province (grant no. 2023-JC-QN-0141), the Qinchuanyuan introducing high-level innovation and entrepreneurship talent program (grant no. QCYRCXM-2022-363), and the Young Talent Support Plan of Xi'an Jiaotong University (grant no. ND6J027).

The article processing charges for this open-access publication were covered by the Helmholtz-Zentrum Hereon.

Review statement. This paper was edited by Arthur Chan and reviewed by two anonymous referees.

References

Abrams, J. Y., Weber, R. J., Klein, M., Sarnat, S. E., Chang, H. H., Strickland, M. J., Verma, V., Fang, T., Bates, J. T., Mulholland, J. A., Russell, A. G., and Tolbert, P. E.: Associations between Ambient Fine Particulate Oxidative Potential and Cardiorespiratory Emergency Department Visits, Environ. Health Perspect., 125, 9, https://doi.org/10.1289/ehp3048, 2017.

Ai, J., Qin, W. H., Chen, J., Sun, Y. W., Yu, Q., Xin, K., Huang, H. Y., Zhang, L. Y., Ahmad, M., and Liu, X. A.: Pollution characteristics and light-driven evolution of environmentally persistent free radicals in $PM_{2.5}$ in two typical northern cities of China, J. Hazard. Mater., 454, 131466, https://doi.org/10.1016/j.jhazmat.2023.131466, 2023.

Ainur, D., Chen, Q. C., Wang, Y. Q., Li, H., Lin, H., Ma, X. Y., and Xu, X.: Pollution characteristics and sources of environmentally persistent free radicals and oxidation potential in fine particulate matter related to city lockdown (CLD) in Xi'an, China, Environ. Res., 210, 11, https://doi.org/10.1016/j.envres.2022.112899, 2022.

Ainur, D., Chen, Q. C., Sha, T., Zarak, M., Dong, Z. P., Guo, W., Zhang, Z. M., Dina, K., and An, T. C.: Outdoor Health Risk of Atmospheric Particulate Matter at Night in Xi'an, Northwestern China, Environ. Sci. Technol., 57, 9252–9265, https://doi.org/10.1021/acs.est.3c02670, 2023.

Alleman, L. Y., Lamaison, L., Perdrix, E., Robache, A., and Galloo, J. C.: PM_{10} metal concentrations and source identification using positive matrix factorization and wind sectoring in a French industrial zone, Atmos. Res., 96, 612–625, https://doi.org/10.1016/j.atmosres.2010.02.008, 2010.

An, J. L., Duan, Q., Wang, H. L., Miao, Q., Shao, P., Wang, J., and Zou, J. N.: Fine particulate pollution in the Nanjing northern suburb during summer: composition and sources, Environ. Monit. Assess., 187, 561, https://doi.org/10.1007/s10661-015-4765-2, 2015.

Arangio, A. M., Tong, H., Socorro, J., Pöschl, U., and Shiraiwa, M.: Quantification of environmentally persistent free radicals and reactive oxygen species in atmospheric aerosol particles, Atmos. Chem. Phys., 16, 13105–13119, https://doi.org/10.5194/acp-16-13105-2016, 2016.

Balakrishna, S., Lomnicki, S., McAvey, K. M., Cole, R. B., Dellinger, B., and Cormier, S. A.: Environmentally persistent free radicals amplify ultrafine particle mediated cellular oxidative stress and cytotoxicity, Part. Fibre Toxicol., 6, 11, https://doi.org/10.1186/1743-8977-6-11, 2009.

Begum, B. A., Biswas, S. K., and Hopke, P. K.: Key issues in controlling air pollutants in Dhaka, Bangladesh, Atmos. Environ., 45, 7705–7713, https://doi.org/10.1016/j.atmosenv.2010.10.022, 2011.

Bhattu, D., Tripathi, S. N., Bhowmik, H. S., Moschos, V., Lee, C. P., Rauber, M., Salazar, G., Abbaszade, G., Cui, T., Slowik, J. G., Vats, P., Mishra, S., Lalchandani, V., Satish, R., Rai, P., Casotto, R., Tobler, A., Kumar, V., Hao, Y., and Qi, L.: Local incomplete combustion emissions define the $PM_{2.5}$ oxidative potential in Northern India, Nat. Commun., 15, 3517, https://doi.org/10.1038/s41467-024-47785-5, 2024.

Borrowman, C. K., Zhou, S. M., Burrow, T. E., and Abbatt, J. P. D.: Formation of environmentally persistent free radicals from the heterogeneous reaction of ozone and polycyclic aromatic compounds, Phys. Chem. Chem. Phys., 18, 205–212, https://doi.org/10.1039/c5cp05606c, 2016.

Brown, S. G., Eberly, S., Paatero, P., and Norris, G. A.: Methods for estimating uncertainty in PMF solutions: Examples with ambient air and water quality data and guidance on reporting PMF results, Sci. Total Environ., 518, 626–635, https://doi.org/10.1016/j.scitotenv.2015.01.022, 2015.

Calas, A., Uzu, G., Kelly, F. J., Houdier, S., Martins, J. M. F., Thomas, F., Molton, F., Charron, A., Dunster, C., Oliete, A., Jacob, V., Besombes, J.-L., Chevrier, F., and Jaffrezo, J.-L.: Comparison between five acellular oxidative potential measurement assays performed with detailed chemistry on PM_{10} samples from the city of Chamonix (France), Atmos. Chem. Phys., 18, 7863–7875, https://doi.org/10.5194/acp-18-7863-2018, 2018.

Campbell, S. J., Wolfer, K., Utinger, B., Westwood, J., Zhang, Z.-H., Bukowiecki, N., Steimer, S. S., Vu, T. V., Xu, J., Straw, N., Thomson, S., Elzein, A., Sun, Y., Liu, D., Li, L., Fu, P., Lewis, A. C., Harrison, R. M., Bloss, W. J., Loh, M., Miller, M. R., Shi, Z., and Kalberer, M.: Atmospheric conditions and composition that influence $PM_{2.5}$ oxidative potential in Beijing, China, Atmos. Chem. Phys., 21, 5549–5573, https://doi.org/10.5194/acp-21-5549-2021, 2021.

Cao, J. J., Wu, F., Chow, J. C., Lee, S. C., Li, Y., Chen, S. W., An, Z. S., Fung, K. K., Watson, J. G., Zhu, C. S., and Liu, S. X.: Characterization and source apportionment of atmospheric organic and elemental carbon during fall and winter of 2003 in Xi'an, China, Atmos. Chem. Phys., 5, 3127–3137, https://doi.org/10.5194/acp-5-3127-2005, 2005.

Charrier, J. G. and Anastasio, C.: Rates of Hydroxyl Radical Production from Transition Metals and Quinones in a Surrogate Lung Fluid, Environ. Sci. Technol., 49, 9317–9325, https://doi.org/10.1021/acs.est.5b01606, 2015.

Chen, Q., Sun, H., Song, W., Cao, F., Tian, C., and Zhang, Y.-L.: Size-resolved exposure risk of persistent free radicals (PFRs) in atmospheric aerosols and their potential sources, Atmos. Chem. Phys., 20, 14407–14417, https://doi.org/10.5194/acp-20-14407-2020, 2020.

Chen, Q. C., Sun, H. Y., Wang, M. M., Wang, Y. Q., Zhang, L. X., and Han, Y. M.: Environmentally Persistent Free Radical (EPFR) Formation by Visible-Light Illumination of the Organic Matter in Atmospheric Particles, Environ. Sci. Technol., 53, 10053–10061, https://doi.org/10.1021/acs.est.9b02327, 2019.

Chen, Q. C., Wang, M. M., Sun, H. Y., Wang, X., Wang, Y. Q., Li, Y. G., Zhang, L. X., and Mu, Z.: Enhanced health risks from exposure to environmentally persistent free radicals and the oxidative stress of $PM_{2.5}$ from Asian dust storms in Erenhot, Zhangbei and Jinan, China, Environ. Int., 121, 260–268, https://doi.org/10.1016/j.envint.2018.09.012, 2018a.

Chen, Q. C., Sun, H. Y., Wang, M. M., Mu, Z., Wang, Y. Q., Li, Y. G., Wang, Y. S., Zhang, L. X., and Zhang, Z. M.: Dominant Fraction of EPFRs from Nonsolvent-Extractable Organic Matter in Fine Particulates over Xi'an, China, Environ. Sci. Technol., 52, 9646–9655, https://doi.org/10.1021/acs.est.8b01980, 2018b.

Comandini, A., Malewicki, T., and Brezinsky, K.: Chemistry of Polycyclic Aromatic Hydrocarbons Formation from Phenyl Radical Pyrolysis and Reaction of Phenyl and Acetylene, J. Phys. Chem. A, 116, 2409–2434, https://doi.org/10.1021/jp207461a, 2012.

Cormier, S. A., Lomnicki, S., Backes, W., and Dellinger, B.: Origin and health impacts of emissions of toxic by-products and fine particles from combustion and thermal treatment of hazardous wastes and materials, Environ. Health Perspect., 114, 810–817, https://doi.org/10.1289/ehp.8629, 2006.

Daellenbach, K. R., Uzu, G., Jiang, J. H., Cassagnes, L. E., Leni, Z., Vlachou, A., Stefenelli, G., Canonaco, F., Weber, S., Segers, A., Kuenen, J. J. P., Schaap, M., Favez, O., Albinet, A., Aksoyoglu, S., Dommen, J., Baltensperger, U., Geiser, M., El Haddad, I., Jaffrezo, J. L., and Prévôt, A. S. H.: Sources of particulate-matter air pollution and its oxidative potential in Europe, Nature, 587, 414–419, https://doi.org/10.1038/s41586-020-2902-8, 2020.

Dalal, N. S., Jafari, B., Petersen, M., Green, F. H. Y., and Vallyathan, V.: Presence of stable coal radicals in autopsied coal miners' lungs and its possible correlation to coal workers' pneumoconiosis, Arch. Environ. Health, 46, 366–372, https://doi.org/10.1080/00039896.1991.9934404, 1991.

Dong, Z., Wang, S. B., Sun, J. B., Shang, L. Q., Li, Z. H., and Zhang, R. Q.: Impact of COVID-19 lockdown on carbonaceous aerosols in a polluted city: Composition characterization, source apportionment, influence factors of secondary formation, Chemosphere, 307, 11, https://doi.org/10.1016/j.chemosphere.2022.136028, 2022.

Dugas, T. R., Lomnicki, S., Cormier, S. A., Dellinger, B., and Reams, M.: Addressing Emerging Risks: Scientific and Regulatory Challenges Associated with Environmentally Persistent Free Radicals, Int. J. Environ. Res. Pu., 13, 17, https://doi.org/10.3390/ijerph13060573, 2016.

Fang, T., Verma, V., Guo, H., King, L. E., Edgerton, E. S., and Weber, R. J.: A semi-automated system for quantifying the oxidative potential of ambient particles in aqueous extracts using the dithiothreitol (DTT) assay: results from the Southeastern Center for Air Pollution and Epidemiology (SCAPE), Atmos. Meas. Tech., 8, 471–482, https://doi.org/10.5194/amt-8-471-2015, 2015.

Fang, T., Lakey, P. S. J., Weber, R. J., and Shiraiwa, M.: Oxidative Potential of Particulate Matter and Generation of Reactive Oxygen Species in Epithelial Lining Fluid, Environ. Sci. Technol., 53, 12784–12792, https://doi.org/10.1021/acs.est.9b03823, 2019.

Fang, T., Hwang, B. C. H., Kapur, S., Hopstock, K. S., Wei, J. L., Nguyen, V., Nizkorodov, S. A., and Shiraiwa, M.: Wildfire particulate matter as a source of environmentally persistent free radicals and reactive oxygen species, Environ. Sci.-Atmospheres, 3, 581–594, https://doi.org/10.1039/d2ea00170e, 2023.

Filippi, A., Sheu, R., Berkemeier, T., Pöschl, U., Tong, H., and Gentner, D. R.: Environmentally persistent free radicals in indoor particulate matter, dust, and on surfaces, Environ. Sci.-Atmospheres, 2, 128–136, https://doi.org/10.1039/d1ea00075f, 2022.

Gao, D., Fang, T., Verma, V., Zeng, L., and Weber, R. J.: A method for measuring total aerosol oxidative potential (OP) with the dithiothreitol (DTT) assay and comparisons between an urban and roadside site of water-soluble and total OP, Atmos. Meas. Tech., 10, 2821–2835, https://doi.org/10.5194/amt-10-2821-2017, 2017.

Gao, D., Mulholland, J. A., Russell, A. G., and Weber, R. J.: Characterization of the water-insoluble oxidative potential of $PM_{2.5}$ using the dithiothreitol assay, Atmos. Environ., 224, 117327, https://doi.org/10.1016/j.atmosenv.2020.117327, 2020.

Gao, J., Huang, J., Li, X., Tian, G., Wang, X., Yang, C., and Ma, C.: Challenges of the UK government and industries regarding emission control after ICE vehicle bans, Sci. Total Environ., 835, 155406, https://doi.org/10.1016/j.scitotenv.2022.155406, 2022.

Gehling, W. and Dellinger, B.: Environmentally Persistent Free Radicals and Their Lifetimes in $PM_{2.5}$, Environ. Sci. Technol., 47, 8172–8178, https://doi.org/10.1021/es401767m, 2013.

Gehling, W., Khachatryan, L., and Dellinger, B.: Hydroxyl Radical Generation from Environmentally Persistent Free Radicals (EPFRs) in $PM_{2.5}$, Environ. Sci. Technol., 48, 4266–4272, https://doi.org/10.1021/es401770y, 2014.

Guo, H. B., Wang, Y. D., Yao, K. X., Zheng, H., Zhang, X. J., Li, R., Wang, N., and Fu, H. Y.: The overlooked formation of environmentally persistent free radicals on particulate matter collected from biomass burning under light irradiation, Environ. Int., 171, 10, https://doi.org/10.1016/j.envint.2022.107668, 2023.

Guo, X. W., Zhang, N., Hu, X., Huang, Y., Ding, Z. H., Chen, Y. J., and Lian, H. Z.: Characteristics and potential inhalation exposure risks of $PM_{2.5}$-bound environmental persistent free radicals in Nanjing, a mega-city in China, Atmos. Environ., 224, 117355, https://doi.org/10.1016/j.atmosenv.2020.117355, 2020.

Heo, J. B., Dulger, M., Olson, M. R., McGinnis, J. E., Shelton, B. R., Matsunaga, A., Sioutas, C., and Schauer, J. J.: Source apportionments of $PM_{2.5}$ organic carbon using molecular marker Positive Matrix Factorization and comparison of results from different receptor models, Atmos. Environ., 73, 51–61, https://doi.org/10.1016/j.atmosenv.2013.03.004, 2013.

Hwang, B., Fang, T., Pham, R., Wei, J. L., Gronstal, S., Lopez, B., Frederickson, C., Galeazzo, T., Wang, X. L., Jung, H., and Shiraiwa, M.: Environmentally Persistent Free Radicals, Reactive Oxygen Species Generation, and Oxidative Potential of Highway $PM_{2.5}$, ACS Earth Space Chem., 5, 1865–1875, https://doi.org/10.1021/acsearthspacechem.1c00135, 2021.

Ikemori, F., Uranishi, K., Asakawa, D., Nakatsubo, R., Makino, M., Kido, M., Mitamura, N., Asano, K., Nonaka, S., Nishimura, R., and Sugata, S.: Source apportionment in $PM_{2.5}$ in central Japan using positive matrix factorization focusing on small-

scale local biomass burning, Atmos. Pollut. Res., 12, 349–359, https://doi.org/10.1016/j.apr.2021.01.006, 2021.

Jang, E., Jeong, T., Yoon, N., and Jeong, S.: Source apportionment of airborne PCDD/F at industrial and urban sites in Busan, South Korea, Chemosphere, 239, 124717, https://doi.org/10.1016/j.chemosphere.2019.124717, 2020.

Jia, H. Z., Zhao, S., Nulaji, G., Tao, K. L., Wang, F., Sharma, V. K., and Wang, C. Y.: Environmentally Persistent Free Radicals in Soils of Past Coking Sites: Distribution and Stabilization, Environ. Sci. Technol., 51, 6000–6008, https://doi.org/10.1021/acs.est.7b00599, 2017.

Jia, S.-M., Wang, D.-Q., Liu, L.-Y., Zhang, Z.-F., and Ma, W.-L.: Size-resolved environmentally persistent free radicals in cold region atmosphere: Implications for inhalation exposure risk, J. Hazard. Mater., 443, 130263, https://doi.org/10.1016/j.jhazmat.2022.130263, 2023.

Jin, L., Xie, J. W., Wong, C. K. C., Chan, S. K. Y., Abbaszade, G., Schnelle-Kreis, J., Zimmermann, R., Li, J., Zhang, G., Fu, P. Q., and Li, X. D.: Contributions of City-Specific Fine Particulate Matter ($PM_{2.5}$) to Differential in Vitro Oxidative Stress and Toxicity Implications between Beijing and Guangzhou of China, Environ. Sci. Technol., 53, 2881–2891, https://doi.org/10.1021/acs.est.9b00449, 2019.

Johnson, K. S., de Foy, B., Zuberi, B., Molina, L. T., Molina, M. J., Xie, Y., Laskin, A., and Shutthanandan, V.: Aerosol composition and source apportionment in the Mexico City Metropolitan Area with PIXE/PESA/STIM and multivariate analysis, Atmos. Chem. Phys., 6, 4591–4600, https://doi.org/10.5194/acp-6-4591-2006, 2006.

Khobragade, P. P. and Ahirwar, A. V.: Source identification and ambient trace element concentrations of PM_{10} using receptor modeling in an urban area of Chhattisgarh, India, Geocarto Int., 37, 12267–12293, https://doi.org/10.1080/10106049.2022.2066201, 2022.

Kim, E. and Hopke, P. K.: Improving source identification of fine particles in a rural northeastern US area utilizing temperature-resolved carbon fractions, J. Geophys. Res.-Atmos., 109, 13, https://doi.org/10.1029/2003jd004199, 2004.

Kundu, S., Kawamura, K., Andreae, T. W., Hoffer, A., and Andreae, M. O.: Diurnal variation in the water-soluble inorganic ions, organic carbon and isotopic compositions of total carbon and nitrogen in biomass burning aerosols from the LBA-SMOCC campaign in Rondonia, Brazil, J. Aerosol Sci., 41, 118–133, https://doi.org/10.1016/j.jaerosci.2009.08.006, 2010.

Lei, M., Huang, X. Z., Wang, C. B., Yan, W. Q., and Wang, S. L.: Investigation on SO_2, NO and NO_2 release characteristics of Datong bituminous coal during pressurized oxy-fuel combustion, J. Therm. Anal. Calorim., 126, 1067–1075, https://doi.org/10.1007/s10973-016-5652-y, 2016.

Li, C., Hakkim, H., Sinha, V., Sinha, B., Pardo, M., Cai, D., Reicher, N., Chen, J., Hao, K., and Rudich, Y.: Variation of $PM_{2.5}$ Redox Potential and Toxicity During Monsoon in Delhi, India, ACS ES&T Air., 1, 316–329, https://doi.org/10.1021/acsestair.3c00096, 2024.

Li, H., Chen, Q. C., Wang, C., Wang, R. H., Sha, T., Yang, X. Q., and Ainur, D.: Pollution characteristics of environmental persistent free radicals (EPFRs) and their contribution to oxidation potential in road dust in a large city in northwest China, J. Hazard. Mater., 442, 130087, https://doi.org/10.1016/j.jhazmat.2022.130087, 2023.

Li, X. Y., Kuang, X. B. M., Yan, C. Q., Ma, S. X., Paulson, S. E., Zhu, T., Zhang, Y. H., and Zheng, M.: Oxidative Potential by $PM_{2.5}$ in the North China Plain: Generation of Hydroxyl Radical, Environ. Sci. Technol., 53, 512–520, https://doi.org/10.1021/acs.est.8b05253, 2019.

Liu, F. and Ng, N. L.: Toxicity of Atmospheric Aerosols: Methodologies & Assays, American Chemical Society, Washington, DC, https://doi.org/10.1021/acsinfocus.7e7012, 2023.

Liu, S. J., Huang, W. L., Yang, J. J., Xiong, Y., Huang, Z. Q., Wang, J. L., Cai, T. T., Dang, Z., and Yang, C.: Formation of environmentally persistent free radicals on microplastics under UV irradiations, J. Hazard. Mater., 453, 10, https://doi.org/10.1016/j.jhazmat.2023.131277, 2023.

Liu, S. T., Liu, G. R., Yang, L. L., Liu, X. Y., Wang, M. X., Qin, L. J., and Zheng, M. H.: Metal-Catalyzed Formation of Organic Pollutants Intermediated by Organic Free Radicals, Environ. Sci. Technol., 56, 14550–14561, https://doi.org/10.1021/acs.est.2c05892, 2022.

Liu, X. Y., Yang, L. L., Liu, G. R., and Zheng, M. H.: Formation of Environmentally Persistent Free Radicals during Thermochemical Processes and their Correlations with Unintentional Persistent Organic Pollutants, Environ. Sci. Technol., 55, 6529–6541, https://doi.org/10.1021/acs.est.0c08762, 2021.

Liu, Y., Wang, R. S., Zhao, T. N., Zhang, Y., Wang, J. H., Wu, H. X., and Hu, P.: Source apportionment and health risk due to PM_{10} and TSP at the surface workings of an underground coal mine in the arid desert region of northwestern China, Sci. Total Environ., 803, 149901, https://doi.org/10.1016/j.scitotenv.2021.149901, 2022.

Nagpure, A. S., Gurjar, B. R., Kumar, V., and Kumar, P.: Estimation of exhaust and non-exhaust gaseous, particulate matter and air toxics emissions from on-road vehicles in Delhi, Atmos. Environ., 127, 118–124, https://doi.org/10.1016/j.atmosenv.2015.12.026, 2016.

Ni, Z., Gao, N., Chen, N., Zhang, C., Liu, Z., Zhu, K. C., Sharma, V. K., and Jia, H. Z.: Particle-size distributions of environmentally persistent free radicals and oxidative potential of soils from a former gasworks site, Sci. Total Environ., 869, 9, https://doi.org/10.1016/j.scitotenv.2023.161747, 2023.

Pryor, W. A., Prier, D. G., and Church, D. F.: Electron-spin resonance study of mainstream and sidestream cigarette smoke: nature of the free radicals in gasphase smoke and in cigarette tar, Environ. Health Perspect., 47, 345–355, https://doi.org/10.1289/ehp.8347345, 1983.

Qin, L. J., Yang, L. L., Yang, J. H., Weber, R., Ranguelova, K., Liu, X. Y., Lin, B. C., Li, C., Zheng, M. H., and Liu, G. R.: Photoinduced formation of persistent free radicals, hydrogen radicals, and hydroxyl radicals from catechol on atmospheric particulate matter, iScience, 24, 102193, https://doi.org/10.1016/j.isci.2021.102193, 2021.

Ramadan, Z., Song, X. H., and Hopke, P. K.: Identification of sources of Phoenix aerosol by positive matrix factorization, J. Air Waste Manage., 50, 1308–1320, https://doi.org/10.1080/10473289.2000.10464173, 2000.

Ramya, C. B., Aswini, A. R., Hegde, P., Boreddy, S. K. R., and Babu, S. S.: Water-soluble organic aerosols over South Asia-

Seasonal changes and source characteristics, Sci. Total Environ., 900, 10, https://doi.org/10.1016/j.scitotenv.2023.165644, 2023.

Reff, A., Eberly, S. I., and Bhave, P. V.: Receptor modeling of ambient particulate matter data using positive matrix factorization: Review of existing methods, J. Air Waste Manage., 57, 146–154, https://doi.org/10.1080/10473289.2007.10465319, 2007.

Runberg, H. L., Mitchell, D. G., Eaton, S. S., Eaton, G. R., and Majestic, B. J.: Stability of environmentally persistent free radicals (EPFR) in atmospheric particulate matter and combustion particles, Atmos. Environ., 240, 117809, https://doi.org/10.1016/j.atmosenv.2020.117809, 2020.

Sarmiento, D. J. and Majestic, B. J.: Formation of Environmentally Persistent Free Radicals from the Irradiation of Polycyclic Aromatic Hydrocarbons, J. Phys. Chem. A, 127, 5390–5401, https://doi.org/10.1021/acs.jpca.3c01405, 2023.

Sharma, S. K., Mandal, T. K., Saxena, M., Sharma, R. A., Datta, A., and Saud, T.: Variation of OC, EC, WSIC and trace metals of PM_{10} in Delhi, India, J. Atmos. Sol.-Terr. Phy., 113, 10–22, https://doi.org/10.1016/j.jastp.2014.02.008, 2014.

Shiraiwa, M., Sosedova, Y., Rouvière, A., Yang, H., Zhang, Y. Y., Abbatt, J. P. D., Ammann, M., and Pöschl, U.: The role of long-lived reactive oxygen intermediates in the reaction of ozone with aerosol particles, Nat. Chem., 3, 291–295, https://doi.org/10.1038/nchem.988, 2011.

Son, Y., Mishin, V., Welsh, W., Lu, S. E., Laskin, J. D., Kipen, H., and Meng, Q. M.: A Novel High-Throughput Approach to Measure Hydroxyl Radicals Induced by Airborne Particulate Matter, Int. J. Environ. Res. Pu., 12, 13678–13695, https://doi.org/10.3390/ijerph121113678, 2015.

Stanimirova, I., Rich, D. Q., Russell, A. G., and Hopke, P. K.: A long-term, dispersion normalized PMF source apportionment of $PM_{2.5}$ in Atlanta from 2005 to 2019, Atmos. Environ., 312, 10, https://doi.org/10.1016/j.atmosenv.2023.120027, 2023.

Tian, L. W., Koshland, C. P., Yano, J. K., Yachandra, V. K., Yu, I. T. S., Lee, S. C., and Lucas, D.: Carbon-Centered Free Radicals in Particulate Matter Emissions from Wood and Coal Combustion, Energ. Fuel., 23, 2523–2526, https://doi.org/10.1021/ef8010096, 2009.

Tong, H. J., Lakey, P. S. J., Arangio, A. M., Socorro, J., Shen, F. X., Lucas, K., Brune, W. H., Pöschl, U., and Shiraiwa, M.: Reactive Oxygen Species Formed by Secondary Organic Aerosols in Water and Surrogate Lung Fluid, Environ. Sci. Technol., 52, 11642–11651, https://doi.org/10.1021/acs.est.8b03695, 2018.

Truong, H., Lomnicki, S., and Dellinger, B.: Potential for Misidentification of Environmentally Persistent Free Radicals as Molecular Pollutants in Particulate Matter, Environ. Sci. Technol., 44, 1933–1939, https://doi.org/10.1021/es902648t, 2010.

Valavanidis, A., Fiotakis, K., Bakeas, E., and Vlahogianni, T.: Electron paramagnetic resonance study of the generation of reactive oxygen species catalysed by transition metals and quinoid redox cycling by inhalable ambient particulate matter, Redox Rep., 10, 37–51, https://doi.org/10.1179/135100005X21606, 2005.

Vejerano, E. P. and Ahn, J.: Leaves are a Source of Biogenic Persistent Free Radicals, Environ. Sci. Tech. Let., 10, 662–667, https://doi.org/10.1021/acs.estlett.3c00277, 2023.

Vejerano, E. P., Rao, G. Y., Khachatryan, L., Cormier, S. A., and Lomnicki, S.: Environmentally Persistent Free Radicals: Insights on a New Class of Pollutants, Environ. Sci. Technol., 52, 2468–2481, https://doi.org/10.1021/acs.est.7b04439, 2018.

Verma, V., Rico-Martinez, R., Kotra, N., King, L., Liu, J. M., Snell, T. W., and Weber, R. J.: Contribution of Water-Soluble and Insoluble Components and Their Hydrophobic/Hydrophilic Subfractions to the Reactive Oxygen Species-Generating Potential of Fine Ambient Aerosols, Environ. Sci. Technol., 46, 11384–11392, https://doi.org/10.1021/es302484r, 2012.

Wang, C., Huang, Y. P., Zhang, Z. T., and Cai, Z. W.: Levels, spatial distribution, and source identification of airborne environmentally persistent free radicals from tree leaves, Environ. Pollut., 257, 11353, https://doi.org/10.1016/j.envpol.2019.113353, 2020.

Wang, C. A., Wang, P. Q., Zhao, L., Du, Y. B., and Che, D. F.: Experimental Study on NO_x Reduction in Oxy-fuel Combustion Using Synthetic Coals with Pyridinic or Pyrrolic Nitrogen, Appl. Sci.-Basel., 8, 12, https://doi.org/10.3390/app8122499, 2018.

Wang, P., Pan, B., Li, H., Huang, Y., Dong, X. D., Ai, F., Liu, L. Y., Wu, M., and Xing, B. S.: The Overlooked Occurrence of Environmentally Persistent Free Radicals in an Area with Low-Rank Coal Burning, Xuanwei, China, Environ. Sci. Technol., 52, 1054–1061, https://doi.org/10.1021/acs.est.7b05453, 2018.

Wang, P. L., Thevenot, P., Saravia, J., Ahlert, T., and Cormier, S. A.: Radical-Containing Particles Activate Dendritic Cells and Enhance Th17 Inflammation in a Mouse Model of Asthma, Am. J. Resp. Cell Mol., 45, 977–983, https://doi.org/10.1165/rcmb.2011-0001OC, 2011.

Wang, S., Ye, J., Soong, R., Wu, B., Yu, L., Simpson, A. J., and Chan, A. W. H.: Relationship between chemical composition and oxidative potential of secondary organic aerosol from polycyclic aromatic hydrocarbons, Atmos. Chem. Phys., 18, 3987–4003, https://doi.org/10.5194/acp-18-3987-2018, 2018.

Wang, Y. D., Yao, K. X., Fu, X., Zhai, X. Y., Jin, L., and Guo, H. B.: Size-resolved exposure risk and subsequent role of environmentally persistent free radicals (EPFRs) from atmospheric particles, Atmos. Environ., 276, 9, https://doi.org/10.1016/j.atmosenv.2022.119059, 2022.

Wang, Y. Q., Li, S. P., Wang, M. M., Sun, H. Y., Mu, Z., Zhang, L. X., Li, Y. G., and Chen, Q. C.: Source apportionment of environmentally persistent free radicals (EPFRs) in $PM_{2.5}$ over Xi'an, China, Sci. Total Environ., 689, 193–202, https://doi.org/10.1016/j.scitotenv.2019.06.424, 2019.

Wang, Y. Q., Wang, M. M., Li, S. P., Sun, H. Y., Mu, Z., Zhang, L. X., Li, Y. G., and Chen, Q. C.: Study on the oxidation potential of the water-soluble components of ambient $PM_{2.5}$ over Xi'an, China: Pollution levels, source apportionment and transport pathways, Environ. Int., 136, 11, https://doi.org/10.1016/j.envint.2020.105515, 2020.

Weichenthal, S., Lavigne, E., Evans, G., Pollitt, K., and Burnett, R. T.: Ambient $PM_{2.5}$ and risk of emergency room visits for myocardial infarction: impact of regional $PM_{2.5}$ oxidative potential: a case-crossover study, Environ. Health, 15, 9, https://doi.org/10.1186/s12940-016-0129-9, 2016.

Xu, Y., Yang, L. L., Wang, X. P., Zheng, M. H., Li, C., Zhang, A. Q., Fu, J. J., Yang, Y. P., Qin, L. J., Liu, X. Y., and Liu, G. R.: Risk evaluation of environmentally persistent free radicals in airborne particulate matter and influence of atmospheric factors, Ecotox. Environ. Safe., 196, 9, https://doi.org/10.1016/j.ecoenv.2020.110571, 2020.

Yang, L. L., Liu, G. R., Zheng, M. H., Jin, R., Zhu, Q. Q., Zhao, Y. Y., Wu, X. L., and Xu, Y.: Highly Elevated Levels and Particle-Size Distributions of Environmentally Persistent Free Radicals in

Haze-Associated Atmosphere, Environ. Sci. Technol., 51, 7936–7944, https://doi.org/10.1021/acs.est.7b01929, 2017.

Yang, Y., Battaglia, M. A., Mohan, M. K., Robinson, E. S., DeCarlo, P. F., Edwards, K. C., Fang, T., Kapur, S., Shiraiwa, M., Cesler-Maloney, M., Simpson, W. R., Campbell, J. R., Nenes, A., Mao, J., and Weber, R. J.: Assessing the Oxidative Potential of Outdoor $PM_{2.5}$ in Wintertime Fairbanks, Alaska, ACS ES&T Air, 1, 175–187, https://doi.org/10.1021/acsestair.3c00066, 2024.

Yi, J.-F., Lin, Z.-Z., Li, X., Zhou, Y.-Q., and Guo, Y.: A short review on environmental distribution and toxicity of the environmentally persistent free radicals, Chemosphere, 340, 139922, https://doi.org/10.1016/j.chemosphere.2023.139922, 2023.

Yu, H. R., Wei, J. L., Cheng, Y. L., Subedi, K., and Verma, V.: Synergistic and Antagonistic Interactions among the Particulate Matter Components in Generating Reactive Oxygen Species Based on the Dithiothreitol Assay, Environ. Sci. Technol., 52, 2261–2270, https://doi.org/10.1021/acs.est.7b04261, 2018.

Yu, Q., Chen, J., Qin, W. H., Ahmad, M., Zhang, Y. P., Sun, Y. W., Xin, K., and Ai, J.: Oxidative potential associated with water-soluble components of $PM_{2.5}$ in Beijing: The important role of anthropogenic organic aerosols, J. Hazard. Mater., 433, 12, https://doi.org/10.1016/j.jhazmat.2022.128839, 2022.

Zhang, X. J., Wang, Y. D., Yao, K. X., Zheng, H., and Guo, H. B.: Oxidative potential, environmentally persistent free radicals and reactive oxygen species of size-resolved ambient particles near highways, Environ. Pollut., 341, 122858, https://doi.org/10.1016/j.envpol.2023.122858, 2024.

Zhao, S., Miao, D., Zhu, K. C., Tao, K. L., Wang, C. Y., Sharma, V. K., and Jia, H. Z.: Interaction of benzo [*a*] pyrene with Cu(II)-montmorillonite: Generation and toxicity of environmentally persistent free radicals and reactive oxygen species, Environ. Int., 129, 154–163, https://doi.org/10.1016/j.envint.2019.05.037, 2019a.

Zhao, S., Gao, P., Miao, D., Wu, L., Qian, Y. J., Chen, S. P., Sharma, V. K., and Jia, H. Z.: Formation and Evolution of Solvent-Extracted and Nonextractable Environmentally Persistent Free Radicals in Fly Ash of Municipal Solid Waste Incinerators, Environ. Sci. Technol., 53, 10120–10130, https://doi.org/10.1021/acs.est.9b03453, 2019b.

Zhong, H., Huang, R.-J., Lin, C., Xu, W., Duan, J., Gu, Y., Huang, W., Ni, H., Zhu, C., You, Y., Wu, Y., Zhang, R., Ovadnevaite, J., Ceburnis, D., and O'Dowd, C. D.: Measurement report: On the contribution of long-distance transport to the secondary aerosol formation and aging, Atmos. Chem. Phys., 22, 9513–9524, https://doi.org/10.5194/acp-22-9513-2022, 2022.